Using 25 GbE Client Rates to Access the Gains of Adaptive Bit- and Code-Rate Networking

David J. Ives, Paul Wright, Andrew Lord, and Seb J. Savory

***Abstract*—For transmission within optical mesh networks, different signal routes acquire different impairments and are received with different signal-to-noise ratios (SNRs). The SNR can be utilized through adaptive bit- and code-rate modulation, which leads to data rates that are not multiples of the preferred 100 GbE client rate. This paper considers the use of slower 25 GbE lanes both with inverse multiplexed 100 GbE client rates and with native 25 GbE client rates and compares network blocking performance. The use of inverse multiplexed 100 GbE client data on four 25 GbE lanes accesses the lion's share of stranded capacity within the network.**

***Index Terms*—Adaptive modulation; Blocking probability; Optical networking.**

I. Introduction

With the ever-increasing amount of traffic on the Internet, there is an urgent need to maximize the load carried by a given optical fiber infrastructure. To this end, the available network resources of bandwidth and transmitted signal signal-to-noise ratio (SNR) must be fully utilized. In a wavelength routed optical network, signals travel a variety of distances and routes and experience a variety of impairments, leading to different signal SNRs. Thus, the theoretical maximum error-free spectral efficiency varies across the network. Contemporary networking has client-side data rates that are fixed, for example, following the Ethernet standard with 100 GbE client data rates such that transport networks are designed to transport multiples of 100 $\mathrm{Gb} \cdot \mathrm{s}^{-1}$ client data.

The variety of transmitted signal SNRs can be fully utilized with adaptive modulation and adaptive forward error correction (FEC) coding [1–5], or alternatively the signal launch power can be adapted to effectively transfer SNR margin between channels to fit the required SNR of an adapted modulation, fixed FEC coding scheme with 100 GbE granularity [6]. The latter requires more complex routing and wavelength assignment algorithms [7] and may not be suitable for sequential or dynamically loaded networks. The former leads to a variety of spectral efficiencies. Elastic bandwidth and flexible grids [8–11] could be used to maintain a fixed client rate by adjusting the symbol rate for a given spectral efficiency, but this again leads to a more complex routing and wavelength assignment and the difficulties of stranded bandwidth.

Thus, we consider the simpler paradigm of a fixed optical grid, fixed optimized launch power, and the use of an adapted modulation and adaptive FEC overhead, leading to a variety of data rates. The use of a fixed grid simplifies the routing and wavelength assignment as each dense WDM (DWDM) channel is now separately constrained. The fixed optimized launch power is obtained for the worst case with the central channel on a fully loaded network. This allows the nonlinear interference to be estimated without knowledge of the future network state [12] and ensures that the established light paths will not be blocked by the acceptance of future demands. The use of the fixed optical grid allows for a small improvement in worst-case nonlinear interference with respect to a flexible grid because the position of the guard bands is known. For a flexible grid, the worst-case nonlinear interference would need to be estimated based on a constant power spectral density without guard bands.

Thus, in general the optimal data rate will not align with the preferred 100 GbE client-side rate, leaving stranded capacity. As pointed out in [13], a flexible Ethernet is required to better match client and optical layers. The recent debates within IEEE 802.3 and the Ethernet community suggest that 25 GbE is a useful data rate that can be transported over single electrical or on–off keying (OOK) optical channels [14,15]. Therefore, to more fully utilize the available data rates of adaptive modulation and adaptive FEC overhead, we consider inverse multiplexing the fixed 100 GbE client rate onto four 25 GbE lanes and transmitting these on the available unused capacity of multiple transceivers.

In this work we simulate the sequential loading of the BT 20 + 2 node UK core network and compare the following:

1) fixed polarization-multiplexed 16 quadrature amplitude modulation (PM-16QAM) and fixed FEC overhead transceivers accepting two-off 100 GbE client demands,

Manuscript received December 2, 2015; revised April 8, 2016; accepted April 29, 2016; published June 3, 2016 (Doc. ID 254761).

D. Ives (e-mail: di231@cam.ac.uk) and S. Savory were with the Optical Networks Group, Department of Electronic and Electrical Engineering, University College London, London, WC1E 7JE, UK, and are now with the Electrical Engineering Division, Department of Engineering, University of Cambridge, 9 JJ Thomson Avenue, Cambridge, CB3 0FA, UK.

A. Lord and P. Wright are with Optical Research, BT Research and Innovation, Adastral Park, Martlesham Heath, Ipswich, IP5 3RE, UK.

http://dx.doi.org/10.1364/JOCN.8.000A86

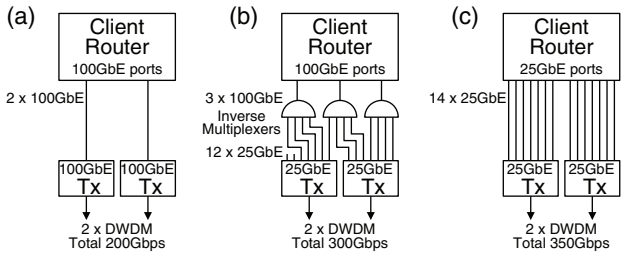

Fig. 1. Transceiver hardware connection options considered: (a) is used with simulation options 1) and 2), (b) is used with simulation option 3), and (c) is used with simulation option 4).

2) adaptive PM m-ary QAM (PM-mQAM) with fixed FEC overhead transceivers accepting multiple 100 GbE client demands in full,
3) adaptive PM-mQAM with adaptive FEC overhead transceivers with 25 GbE lanes with 100 GbE client demands inverse multiplexed onto 25 GbE lanes and accepted on a single or across multiple transceivers,
4) adaptive PM-mQAM with adaptive FEC overhead transceivers with multiple 25 GbE client demands accepted in full.

These transceiver options are illustrated in Fig. 1. The final option is included to take full advantage of the finer granularity and is expected to show the best performance. We compare these options on blocking performance and on the number of transceivers required to transport a given network load. We also suggest how the transceiver options must be priced in order to economically increase the data transmission within the network considered here.

II. Impairment Adaptive Modulation and Coding

We consider a network using polarization-multiplexed coherent optical communications such that linear impairments are equalized in the receiver, and signal transmission quality is limited by amplified spontaneous emission (ASE) noise and nonlinear interference (NLI). We assume that NLI can be calculated using the incoherent Gaussian noise (GN) model [16] and consider an egalitarian operation [12] where all the DWDM channels are assumed equally power loaded and the NLI of the worst-case central DWDM channel is assumed for all DWDM channels. The transmission signal symbol SNR can be written as

$$\mathrm{SNR} = \frac{p}{\sum_i \mathrm{ASE}_i + p^3 \sum_j X(L_j)}, \tag{1}$$

where p is the signal launch power of each DWDM channel, ASE_i is the ASE noise power from the ith erbium-doped fiber amplifier (EDFA), and $X(L_j)$ is a NLI factor describing the NLI on the worst-case central DWDM channel for the jth span of length L_j. All the noise powers are measured within the receivers' matched filter bandwidth. The summations i and j are over all EDFAs and fiber spans, respectively, along the optical transmission route.

The ASE noise within the receivers' matched filter bandwidth is given by

$$\mathrm{ASE}_i = 10^{\frac{\mathrm{NF}}{10}} h\nu 10^{\frac{A_i}{10}} R, \tag{2}$$

where NF is the amplifier noise figure taken as 4.5 dB, h is Planck's constant, ν is the optical carrier frequency 193.5 THz, R is the symbol rate (baud), and A_i is the loss between the $(i-1)$th and the ith amplifier (dB), which will be fully compensated by the ith amplifier. The EDFAs were assumed to be equally spaced within a link with a maximum spacing of 60 km. All the reconfigurable optical add–drop multiplexer (ROADM) nodes were assumed to have 22 dB loss compensated by a following EDFA.

$X(L)$ was obtained by numerical integration of the GN model over the full c-band with 100 channels spaced at 50 GHz and across the channel matched filter $H(f)$. $X(L)$ is given by

$$X(L) = \frac{16}{27}\gamma^2 \int_{-\infty}^{\infty}\int_{-\infty}^{\infty}\int_{-\infty}^{\infty} g(f_1)g(f_2)g(f_1+f_2-f)H(f) \times \frac{1+e^{-2\alpha L}-2e^{-\alpha L}\cos[4\pi^2\beta_2(f_1-f)(f_2-f)L]}{\alpha^2+[4\pi^2\beta_2(f_1-f)(f_2-f)]^2}\mathrm{d}f_1\mathrm{d}f_2\mathrm{d}f, \tag{3}$$

where the spans were assumed to be standard single-mode fiber (SSMF) with attenuation of 0.25 $\mathrm{dB\cdot km^{-1}}$, $\alpha = 0.0576\,\mathrm{km^{-1}}$, chromatic dispersion, $\beta_2 = -21.3\,\mathrm{ps^2\cdot km^{-1}}$, and nonlinear coefficient $\gamma = 1.3\ \mathrm{W^{-1}\cdot km^{-1}}$. The total signal power spectral density is given by $p \times g(f)$ where the normalized power spectral density $g(f)$ is given by

$$g(f) = \frac{1}{R}\sum_{i=-50}^{49} \mathrm{rect}\left(\frac{f+i*\Delta f}{R}\right), \tag{4}$$

where R is the symbol rate of 32 Gbaud, Δf is the DWDM channel spacing of 50 GHz, and $\mathrm{rect}(x)$ is the rectangle function such that $\mathrm{rect}(x) = 1$ for $-0.5 < x < 0.5$ and 0 elsewhere. The matched filter $H(f)$ is given by

$$H(f) = \mathrm{rect}\left(\frac{f}{R}\right). \tag{5}$$

For the BT 20 + 2 node UK core network of Fig. 4 below, the span lengths vary considerably, and thus an analytic estimation of $X(L)$ was developed to accurately capture the span length dependence and avoid repeated numerical integration as

$$X(L) = X(\infty)[1-\mathrm{e}^{a_0 L}]^{a_1}, \tag{6}$$

where $X(\infty) = 8.26231\times10^{-4}\ \mathrm{mW^2\cdot span^{-1}}$ is the NLI factor for an infinitely long span obtained by numerical integration of the GN model, and a_0 and a_1 were found to be $0.0987595\ \mathrm{km^{-1}}$ and 1.190506, respectively, by fitting the numerical data to minimize the sum of squares of the error between the analytic equation and the numerical results. The numerically integrated and analytical estimations of $X(L)$ are compared in Fig. 2, where the RMS difference

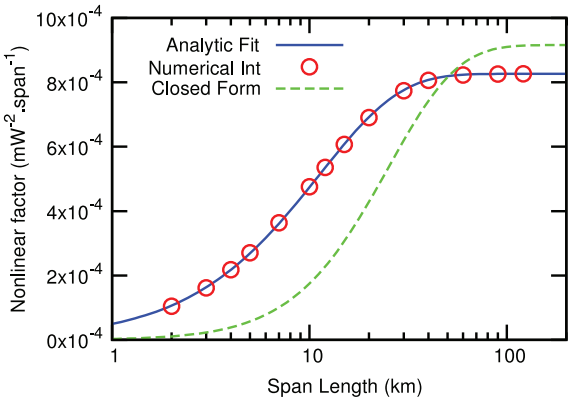

Fig. 2. Nonlinear interference factor $X(L)$ versus span length.

was found to be 1.3×10^{-6} mW$^{-2} \cdot$ span^{-1}. Also shown in Fig. 2 is the closed form GN model of Poggiolini {Eq. (39) in [17]}, illustrating that while this is within 0.5 dB of the numerical integrated values for long span lengths, there is a large discrepancy at shorter span lengths.

For a given symbol SNR, the modulation format and FEC overhead were chosen to maximize the data throughput. We consider ideal hard decision FEC where, for a pre-FEC BER P_b, the maximum code rate r_c that results in error-free transmission is given by [18]

$$r_c = 1 + P_b \log_2[P_b] + (1 - P_b)\log_2[1 - P_b], \tag{7}$$

such that for polarization-multiplexed quaternary phase-shift keying (PM-QPSK) modulation at 32 Gbaud, the maximum error-free information rate is $32 \times 4 \times r_c$ Gb $\cdot$ s^{-1}. We allow a 5% overhead for the OTU framing, leading to a maximum client data rate of $\frac{1}{1.05} 32 \times 4 \times r_c$ Gb $\cdot$ s^{-1} for the PM-QPSK modulation.

We actually solve the reverse of this, that is, for a given data rate, we choose the modulation format and FEC overhead to minimize the required SNR for error-free transmission. The data rates are chosen to be in multiples of 25 GbE with 5% framing OH, giving a data rate granularity of 26.25 Gb $\cdot$ s^{-1}. Thus, for each modulation format, the required code rate can be calculated thence from Eq. (7), the required pre-FEC BER P_b can be found, and finally the required SNR to achieve this pre-FEC BER can be calculated given the modulation format. The required SNR for client data rates on 100 and 25 Gb $\cdot$ s^{-1} lanes transported using PM-QPSK, PM-16QAM, PM-64QAM, and PM-256QAM are shown in Table I and illustrated in Fig. 3.

III. Sequential Loaded Network Simulations

To demonstrate the gains by fully utilizing the available SNR, sequential loading of the BT 20 + 2 node UK core network was considered. Figure 4 shows the network topology and link lengths used. The subset of modulation format/code rate combinations utilized in a given network depends on the range of SNR for the light paths within that network [19]. Larger diameter networks will utilize a subset of lower data rate combinations, while smaller diameter networks will use higher data rate combinations. For both cases the granularity of the data rate with SNR is 25 Gb $\cdot$ s^{-1}; the advantage of the finer granularity is what this work explores, and thus similar conclusions are expected for other networks.

TABLE I
Modulation Formats, Data Rates, and Required Symbol SNRs for the 32 Gbaud Signals Used

Modulation Format	Code Rate	Information (Gb $\cdot$ s^{-1})	Client Data (Gb $\cdot$ s^{-1})	Required SNR (dB)
PM-QPSK	0.41	52.5	50	0.59
PM-QPSK	0.62	78.8	75	3.16
PM-QPSK	0.82	105.0	100	5.69
PM-16QAM	0.49	131.3	125	7.63
PM-16QAM	0.62	157.5	150	9.14
PM-16QAM	0.72	183.8	175	10.58
PM-16QAM	0.82	210.0	200	12.08
PM-16QAM	0.92	236.3	225	14.06
PM-64QAM	0.68	262.5	250	15.45
PM-64QAM	0.75	288.8	275	16.57
PM-64QAM	0.82	315.0	300	17.73
PM-64QAM	0.89	341.3	325	19.07
PM-64QAM	0.96	367.5	350	20.85
PM-256QAM	0.77	393.8	375	22.24
PM-256QAM	0.82	420.0	400	23.23
PM-256QAM	0.87	446.3	425	24.29
PM-256QAM	0.92	472.5	450	25.53

Uniformly random demands were sequentially added to the network in the following way. If a transceiver with sufficient unused capacity was available between the source and destination nodes, then the demand was accepted in full by that transceiver. If a transceiver was available between the source and destination nodes with insufficient unused capacity to fully accept the demand and a new transceiver can be set up following the same path, the demand was accepted across the two transceivers. Otherwise a new light path was routed using the congestion aware shortest path (number of hops) based on [18] and, if the DWDM spectrum was available, the first fit wavelength

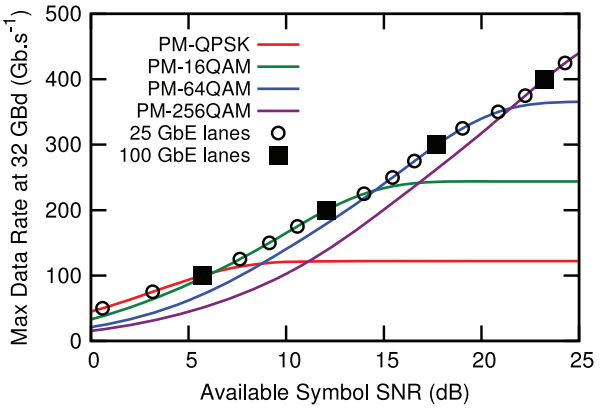

Fig. 3. Client data rate versus symbol SNR for various code rate and modulation formats.

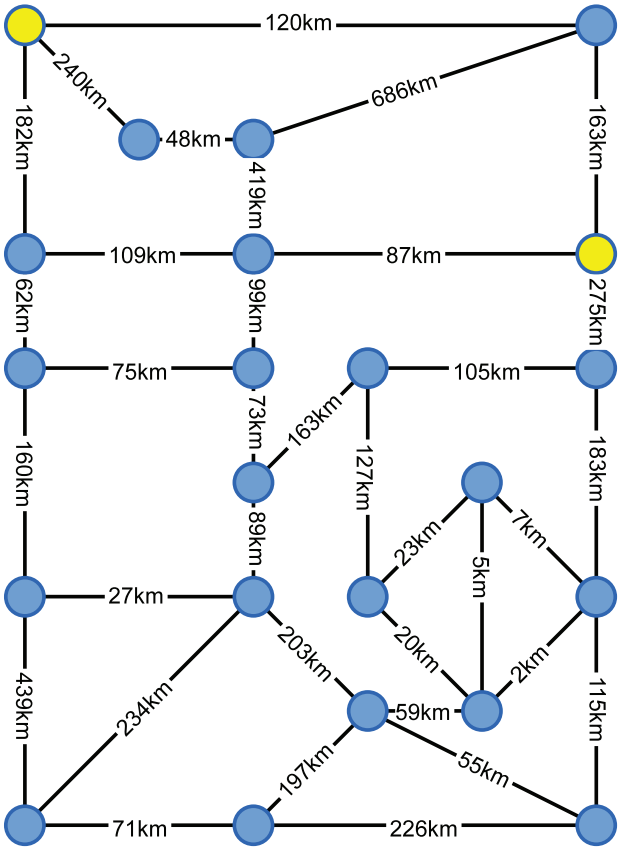

Fig. 4. BT 20 + 2 node UK core topology showing link lengths in kilometers (km). The two yellow nodes did not supply or receive traffic and are for routing purposes only.

chosen to activate the transceiver. The SNR of the available route was calculated and the highest capacity signal format chosen from Table I where the route SNR exceeds the required SNR for error-free transmission. The demand was accepted onto the new transceiver. If all these options failed, then the demand was deemed to have been blocked. The process of routing and accepting a demand is illustrated in the flow chart of Fig. 5.

Either 2000, 100 $\mathrm{Gb \cdot s^{-1}}$ or 8000, 25 $\mathrm{Gb \cdot s^{-1}}$ bi-directional demands, a total of 400 $\mathrm{Tb \cdot s^{-1}}$, were imposed on the network and the accumulation of blocking and number of active transceivers was recorded. The simulation was repeated 10,000 times, and the mean accumulated blocking was calculated to improve the statistics. The cumulative blocking probability after the ith demand CBP_i was calculated as

$$\mathrm{CBP}_i = \frac{\mathrm{Block}_i}{i}, \tag{8}$$

where Block_i is the mean accumulated blocking after the ith demand. The mean accepted network load after the ith demand is thus $i(1 - \mathrm{CBP}_i)$, and the probability that the next demand will be blocked (BP_i) was calculated from the cumulative blocking probability as

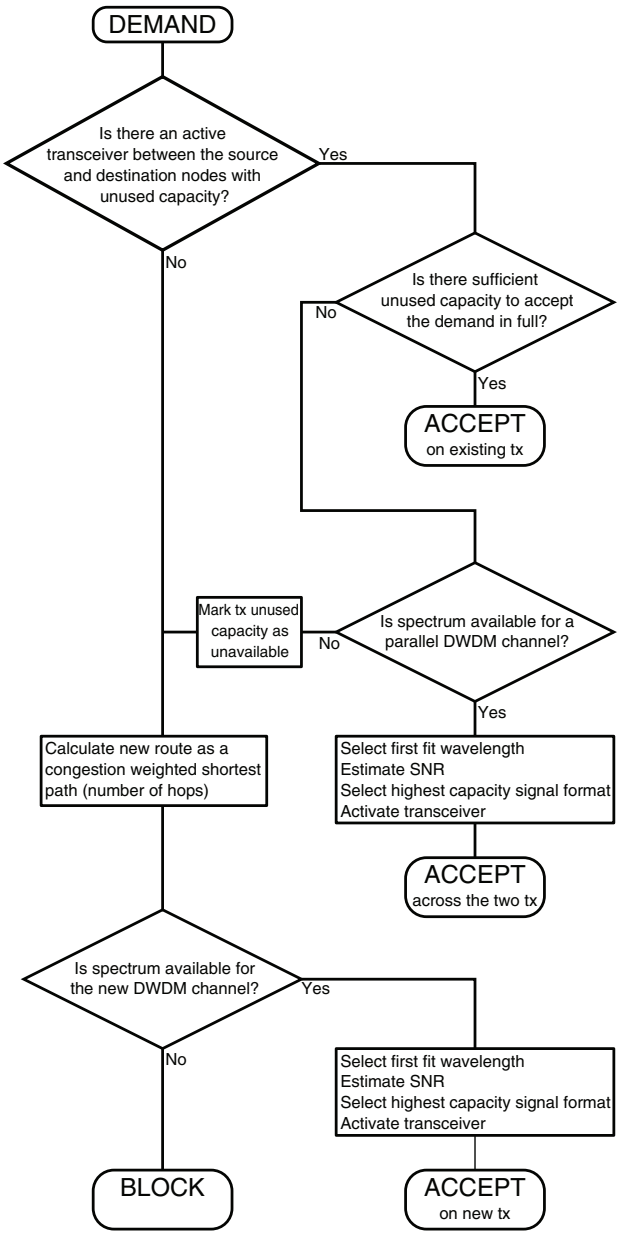

Fig. 5. Process of routing and accepting sequential demands.

$$\mathrm{BP}_i = (i+1)\mathrm{CBP}_{i+1} - i\mathrm{CBP}_i. \tag{9}$$

The network load that gives a 1% blocking probability was calculated by linearly fitting the blocking probability versus load in the log domain over a blocking probability range of 0.5% to 2%. The 0.1% and 10% blocking probabilities were also calculated by fitting over 0.05% to 0.2% and 6% to 15%, respectively. The simulation was carried out for the four different transceiver configurations described in Section I and illustrated in Fig. 1.

Figure 6 shows the blocking probability versus accepted load for the different transceiver configurations described above. The network loads at 0.1%, 1%, and 10% blocking probabilities are shown in Table II and increase from

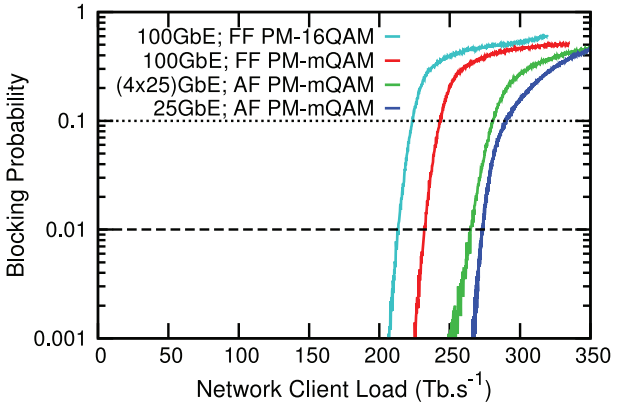

Fig. 6. Blocking probability versus network load for the BT 20 + 2 node UK core network. For the four transceiver configurations considered, FF = fixed FEC-OH, and AF = adaptive FEC-OH.

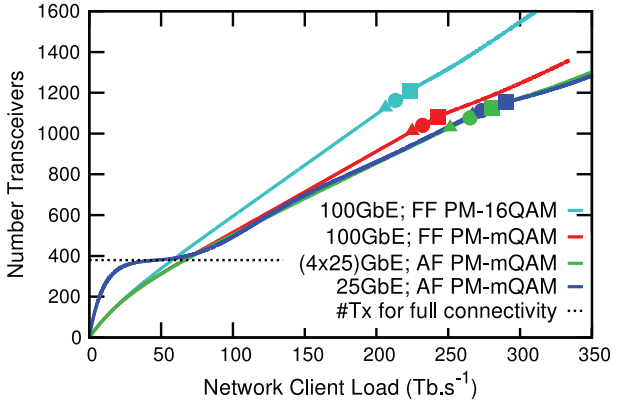

Fig. 7. Number of active transceivers versus network load for the BT 20 + 2 node UK core network. For the four transceiver configurations considered, FF = fixed FEC-OH, and AF = adaptive FEC-OH. The triangle, circle, and square symbols correspond to blocking probabilities of 0.1%, 1%, and 10%, respectively. The dotted line indicates 380 transceivers, the minimum required to fully connect the network.

213.3 to 273.3 Tb · s^{-1} for 1% blocking in going from fixed PM-16QAM with fixed FEC overhead and 100 GbE demands to adapted PM-mQAM with adapted FEC overhead and 25 GbE demands. For transceivers with 100 GbE client data granularity, the stranded capacity will range from 0 to <100 Gb · s^{-1}, and thus it is expected that on average 50 Gb · s^{-1} per transceiver of client data capacity will be stranded by incomplete utilization of the available SNR. Given that approximately 1000 transceivers are active, 50 Tb · s^{-1} of client data capacity is unused. This stranded capacity will fall to an average of 50 Gb · s^{-1} per node pair when the demands are inverse multiplexed onto 25 GbE lanes, a total of 19 Tb · s^{-1}, and fall further to 12.5 Gb · s^{-1} per transceiver when 25 GbE client demands are used, a total of just 12.5 Tb · s^{-1}. This view is consistent with the results shown in Fig. 6 and suggests that moving to 100 GbE demands split across four 25 GbE lanes gives the lion's share of capacity improvement.

Figure 7 shows the evolution of the number of active transceivers in the network as the network load is increased for the four different transceiver configurations. The point at which 0.1%, 1%, and 10% blocking probabilities occur are marked by triangle, circle, and square symbols, respectively. By using adaptive modulation and adaptive FEC overhead, it can be seen that fewer transceivers are required at the higher network loads. It also shows that at higher loads 100 GbE demands split across four 25 GbE lanes utilizes approximately the same number of transceivers as using 25 GbE demands directly, but suffers slightly earlier blocking. At low network loads, the use of 25 GbE demands shows that significantly more transceivers are required for a given network load. Near zero load, the number of transceivers required increases with the number of demands such that for 25 GbE demands, the number of transceivers will increase four times faster than for 100 GbE demands by a given load. This initial rise continues until there are 380 transceivers, enough to fully connect the network, then the unused capacity on the transceivers is used to accommodate further demands, leading to a plateau in the number of transceivers required. This low load regime is not an area of interest for future optical networking.

By comparing the number of transceivers used at the higher network load of 200 Tb · s^{-1}, it is possible to estimate the break-even economic price for the different transceiver technologies. The final column of Table II shows the average number of transceivers used to accept the load of 200 Tb · s^{-1} under the four different transceiver configurations considered. For the technology to be economically acceptable, the price of including adaptive format technology needs to be less than 20% greater than a fixed PM-16QAM transceiver, and the price of including adaptive FEC overhead should not increase the transceiver price

TABLE II
NETWORK LOAD FOR A NUMBER OF BLOCKING PROBABILITIES AND THE NUMBER OF ACTIVE TRANSCEIVERS AT A NETWORK LOAD OF 200 Tb · s^{-1} FOR THE FOUR TRANSCEIVER CONFIGURATIONS CONSIDERED

	Network Load (Tb · s^{-1}) for Blocking Probability			No. Tx at Load
Transceiver Configuration	0.1%	1%	10%	200 Tb · s^{-1}
Fixed PM-16QAM fixed FEC-OH GbE demands	206.4	213.3	223.4	1095
Adaptive PM-mQAM fixed FEC-OH GbE demands	224.8	232.1	243.1	913
Adaptive PM-mQAM adaptive FEC-OH GbE demands	251.4	265.1	280.7	854
Adaptive PM-mQAM adaptive FEC-OH GbE demands	266.9	273.3	290.0	861

by more than 6% above that of a fixed FEC coded adaptive modulation transceiver. This final 6% must also include the cost of any electronic switches required to convert the 100 GbE signals into multiple 25 GbE signals and connect them to multiple transceivers.

IV. Conclusions

This paper has considered the problem of fully utilizing the available SNR resource in a sequentially loaded mesh network. The use of adaptive modulation formats and adaptive FEC overhead can access the available capacity, but leads to transceiver capacities that are not multiples of the currently preferred client data rate.

We show through sequential loading of the BT 20 + 2 node UK core network that by inverse multiplexing 100 GbE demands onto four 25 GbE lanes that can be split across multiple transceivers, the majority of the stranded capacity can be utilized.

We also compare the number of transceivers required to support a given network load and conclude that for such technologies to be economically viable within the BT 20 + 2 node UK core network, the transceivers capable of adaptive modulation format must cost no more than 20% more than fixed PM-16QAM transceivers, and the adaptive FEC overhead must add no more than 6% to the price of the transceivers capable of adaptive modulation format.

V. Data Access

Additional data related to this publication is available at the University of Cambridge data repository: https://www.repository.cam.ac.uk/handle/1810/255993.

Acknowledgment

The authors acknowledge support from the UK Engineering and Physical Sciences Research Council (EPSRC) through the project grant INSIGHT, EP/L026155/1, and the programme grant UNLOC, EP/J017582/1; from The Royal Academy of Engineering/The Leverhulme Trust; and also from the EU Seventh Framework Programme (FP7) through the IDEALIST project No. 317999.

References

[1] G.-H. Gho and J. M. Kahn, "Rate-adaptive modulation and coding for optical fiber transmission systems," *J. Lightwave Technol.*, vol. 30, no. 12, pp. 1818–1828, June 2012.

[2] M. Arabaci, I. B. Djordjevic, L. Xu, and T. Wang, "Nonbinary LDPC-coded modulation for rate-adaptive optical fiber communication without bandwidth expansion," *IEEE Photonics Technol. Lett.*, vol. 24, no. 16, pp. 1402–1404, Aug. 2012.

[3] L. Potì, G. Meloni, G. Berrettini, F. Fresi, M. Secondini, T. Foggi, and G. Colavolpe, "Casting 1 Tb/s DP-QPSK communication into 200 GHz bandwidth," in *European Conf. on Optical Communication*, Brussels, Belgium, 2012, paper P4.19.

[4] D. A. A. Mello, A. N. Barreto, T. C. de Lima, T. F. Portela, L. Beygi, and J. M. Kahn, "Optical networking with variable-code-rate transceivers," *J. Lightwave Technol.*, vol. 32, no. 2, pp. 257–266, Jan. 2014.

[5] A. Alvarado, D. J. Ives, S. J. Savory, and P. Bayvel, "On optimal modulation and FEC overhead for future optical networks," in *Optical Fiber Communication Conf.*, Los Angeles, CA, 2015, paper Th3E.1.

[6] D. J. Ives, P. Bayvel, and S. J. Savory, "Assessment of options for utilizing SNR margin to increase network data throughput," in *Optical Fiber Communication Conf.*, Los Angeles, CA, Mar. 2015, paper M2I.3.

[7] D. J. Ives, P. Bayvel, and S. J. Savory, "Physical layer transmitter and routing optimization to maximize the traffic throughput of a nonlinear optical mesh network," in *Optical Network Design and Modeling*, Stockholm, Sweden, May 2014, pp. 168–173.

[8] M. Jinno, H. Takara, B. Kozicki, Y. Tsukishima, Y. Sone, and S. Matsuoka, "Spectrum-efficient and scalable elastic optical path network: Architecture, benefits, and enabling technologies," *IEEE Commun. Mag.*, vol. 47, no. 11, pp. 66–73, Nov. 2009.

[9] O. Gerstel, M. Jinno, A. Lord, and S. J. B. Yoo, "Elastic optical networking: A new dawn for the optical layer?" *IEEE Commun. Mag.*, vol. 50, no. 2, pp. s12–s20, Feb. 2012.

[10] F. Fresi, "Self-adaptation technique for bandwidth-variable transponders," in *Photonics in Switching*, 2015, pp. 157–159.

[11] F. Cugini, F. Paolucci, F. Fresi, G. Meloni, N. Sambo, L. Potì, A. D'Errico, and P. Castoldi, "Toward plug-and-play software-defined elastic optical networks," *J. Lightwave Technol.*, vol. 34, no. 6, pp. 1494–1500, Mar. 2016.

[12] D. J. Ives, A. Lord, P. Wright, and S. J. Savory, "Quantifying the impact of non-linear impairments on blocking load in elastic optical networks," in *Optical Fiber Communication Conf.*, San Francisco, CA, Mar. 2014, paper W2A.55.

[13] X. Zhao, V. Vusirikala, B. Koley, V. Kamalov, and T. Hofmeister, "The prospect of inter-data-center optical networks," *IEEE Commun. Mag.*, vol. 51, no. 9, pp. 32–38, Sept. 2013.

[14] 25 Gb/s Ethernet Task Force, IEEE P802.3, 2015 [Online]. Available: http://www.ieee802.org/3/by.

[15] 25 Gigabit Ethernet Consortium [Online]. Available: http://25gethernet.org.

[16] P. Poggiolini, "The GN model of non-linear propagation in uncompensated coherent optical systems," *J. Lightwave Technol.*, vol. 30, no. 24, pp. 3857–3879, Dec. 2012.

[17] P. Poggiolini, "The GN-model of fiber non-linear propagation and its applications," *J. Lightwave Technol.*, vol. 32, no. 4, pp. 694–721, Feb. 2014.

[18] S. J. Savory, "Congestion aware routing in nonlinear elastic optical networks," *IEEE Photonics Technol. Lett.*, vol. 26, no. 10, pp. 1057–1060, May 2014.

[19] A. Alvarado, D. J. Ives, S. J. Savory, and P. Bayvel, "On the impact of optimal modulation and FEC overhead on future optical networks," *J. Lightwave Technol.*, vol. 34, no. 9, pp. 2339–2352, May 2016.